

# Vibration analysis of new drill string system with hydro-oscillator in horizontal well<sup>†</sup>

Jialin Tian<sup>1,2</sup>, Zhi Yang<sup>1,\*</sup>, You Li<sup>1</sup>, Lin Yang<sup>1</sup>, Chunming Wu<sup>1</sup>, Gang Liu<sup>1</sup> and Changfu Yuan<sup>1</sup>

<sup>1</sup>School of Mechatronic Engineering, Southwest Petroleum University, Chengdu, 610500, China

<sup>2</sup>School of Mechanical Engineering, Southwest Jiaotong University, Chengdu, 610031, China

(Manuscript Received July 18, 2015; Revised December 8, 2015; Accepted February 21, 2016)

## Abstract

With the growth of oil and gas resource demand, the hydro-oscillator is widely used to enhance the Rate of penetration (ROP) and improve the efficacy in drilling various wells. The vibration model is the key issue of dynamics analysis and optimization of downhole tools. For the vibration analysis of the new drill string system with hydro-oscillator in the horizontal well, based on the design of the new hydro-oscillator and its operation conditions, the kinematics expressions are presented. Combined with the vibration force calculation results of the hydro-oscillator, the dynamics model of the new drill string system is established. Furthermore, the important features of vibration frequency, displacement, velocity and acceleration are discussed in the numerical example calculation results. By comparing the results of the calculation and experiment test, we can verify the correctness of the analysis model. With the hydro-oscillator vibration effect, the static friction between the drill string and wellbore is changed to the dynamic friction, so it can result in a significant increase in run length. At the same time, the ROP can be enhanced with the vibration effect. Moreover, with the parameters' adjustment according to the operation conditions, the analysis method and model can also provide references to the study of similar downhole tools dynamics or mechanical properties.

**Keywords:** Drilling; Hydro-oscillator; Drill string; Vibration; Horizontal well; ROP

## 1. Introduction

With the growth of oil and gas resource demand, drilling engineering faces more complex operation conditions [1, 2]. For example, directional drilling or ERD (Extended reach drilling) is widely used in oil and gas mining field; with the increasing development of well drilling towards deep layers, high temperature and complex tracking, it produces some new challenges. To a directional or horizontal well, the friction between the drill string and wellbore has become the key factor of reducing the ROP, which makes the Weight on bit (WOB) loss and low rock-breaking efficiency [3]. To solve the above problem, scholars in related fields have done much research [4-7]. Compared with other methods and technologies, downhole vibration or shock tools [8-13] can make drill string produce certain frequency and amplitude of periodic vibration, which can obviously reduce frictional resistance, improve drilling ROP and shorten drilling time.

The hydro-oscillator is a typical downhole tool which uses self-generated vibration to improve WOB transfer and decreases friction between drill string and wellbore efficiently. Furthermore, it has good adaptability in different and complex

drilling patterns. For its simple and effective work model, the hydro-oscillator quickly attracts the oil industry's eyes and has been successfully applied in many field sites. Unfortunately, to the best of our knowledge, for the complexity of drilling parameters, the existing research has focused on experimental or field tests, and did not make a detailed study on the tool working mechanism, theory model or vibration characteristics [14-18].

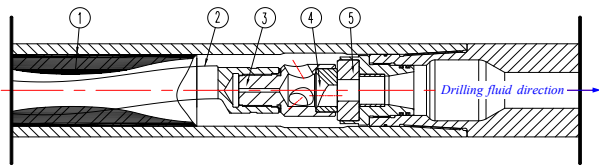
Therefore, this paper is devoted to a novel hydro-oscillator introduction and its vibration analysis in a horizontal drill string system, which provides a deep insight into the engineering applications. The rest of this paper is organized as follows: In Sec. 2, the design of new hydro-oscillator is introduced and the vibration of the new drill string system with the hydro-oscillator in the horizontal well is analyzed, including the kinematics expressions and dynamics model. The analysis method and models can also provide reference for the study of similar downhole tools dynamics or mechanical properties. Sec. 3 carries out the numerical calculation and analysis of the vibration system, including important parameters such as displacement, velocity and acceleration. In Sec. 4, the laboratory experiment is designed according to the example parameters, and the results from the example and experiment verifies the rationality of the vibration analysis model. Finally, some conclusions are summarized.

\*Corresponding author. Tel.: +86 13882236886

E-mail address: 309009838@qq.com

<sup>†</sup>Recommended by Associate Editor Eung-Soo Shin

© KSME & Springer 2016



① Stator; ② Rotor; ③ Adapter; ④ Dynamic valve plate; ⑤ Static valve plate

Fig. 1. Design of the hydro-oscillator.

## 2. Hydro-oscillator design and analysis model

### 2.1 Hydro-oscillator design

Considering the drilling field conditions, the new hydro-oscillator is designed as shown in Fig. 1, consisting of the Positive displacement motor (PDM) including the stator and rotor ②, adapter ③ with three branch holes, dynamic valve plate ④ and static valve plate ⑤, etc.

The hydro-oscillator is assembled with the shock absorber, and the oscillator is at the side of near the drill bit. Under the downhole operation conditions, the drilling fluid flows through the rotor and stator, and the rotor movement determines the motion of the adapter and dynamic valve plate. Therefore, the flow area between the dynamic and static valve plate produces periodic change, which results in a periodic change of drilling fluid pressure. Coupled with the Bottom hole assembly (BHA) including the drill bit, hydro-oscillator and absorber, the pressure energy of drilling fluid turns into the mechanical energy of drill string, which causes the vibration of downhole tools.

### 2.2 Kinematic characteristics of hydro-oscillator

To analyze the vibration characteristics of the hydro-oscillator, the kinematic characteristics must be first determined. Rather, according to the working mechanism of this new tool, the change rule of the flow area between the dynamic and static valve plate is the key issue to solve the kinematic characteristics of the tool.

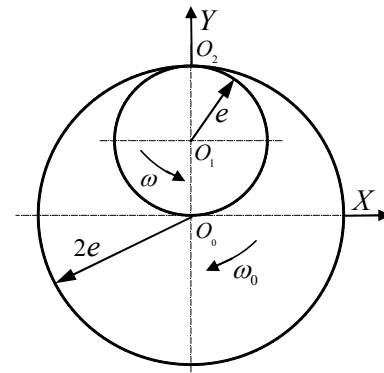
First, the study of the screw motor movement features is the foundation of the hydro-oscillator kinematic analysis. For the need of high speed and small torque, the lobe configuration is 1:2, which is different from the normal configuration in most drilling motors. Setting the conjugate profile of the motor as hypocycloidal curve, the expressions of flow quantity of per revolution  $q$ , the sectional area of stator  $A_s$ , and the sectional area of rotor  $A_r$ , can be described by

$$q = (A_s - A_r)NT_s = 8eD_r h \tag{1}$$

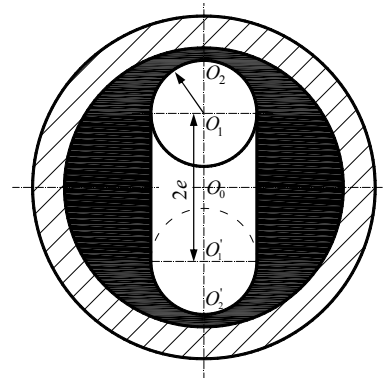
$$A_s = \pi R^2 + 8eR \tag{2}$$

$$A_r = \pi R^2 \tag{3}$$

where  $N$  is the rotor ends lobes and here  $N = 1$ ,  $T_s$  is the stator lead,  $e$  is the rotor eccentricity value,  $D_r$  is the external diame-



(a) Motion characteristics of the rotor  $O_1$



(b) Sectional drawing of the rotor moved in the stator

Fig. 2. Kinematic relationship of the rotor and stator.

ter of the stator,  $h$  is the motor screw pitch, and  $R$  is the rotor radius.

Moreover, for the hydro-oscillator, the rotor motion can be described as a circle with center  $O_1$  and radius  $e$ , pure rolling in another circle with center  $O_0$  and radius  $2e$ . The movement and position relationship is shown in Fig. 2(a). Defining  $\omega$  as the rotation angular velocity of the rotor around its center  $O_1$ ,  $\omega_0$  as the revolution angular velocity of the rotor center  $O_1$  around the stator center  $O_0$ ,  $\omega$  can be given as

$$\omega = 2\pi \frac{Q\eta_v}{q} \tag{4}$$

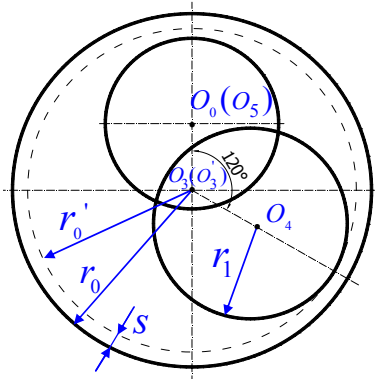
where  $Q$  is the total flow rate,  $\eta_v$  is the flow efficiency. The relationship between  $\omega$  and  $\omega_0$  can be obtained as

$$\omega = -\omega_0 \tag{5}$$

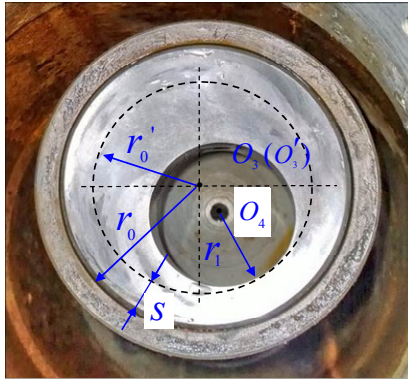
As for the center  $O_1$ , its motion trajectory is a straight line in Fig. 2(b). After a certain time  $t$  and for Eq. (5), the rotation angle  $\theta$  of the rotor center  $O_1$  is

$$\theta = \omega t \tag{6}$$

Defining the point  $O_2$  as one point on the circle  $O_1$ , the coordinate equation of  $O_2$  can be described as



(a) Structural drawings of the dynamic valve plate



(b) Real photo of the dynamic valve plate

Fig. 3. Parameters relationship on the dynamic valve plate.

$$\begin{cases} x_2 = 0 \\ y_2 = 2e \cos \omega t \end{cases} \quad (7)$$

where  $E$  is the rotor eccentricity, which equals to the displacement between  $O_0$  and  $O_1$ .

For connecting with the adapter and rotor, the dynamic valve plate is the same movement features with the rotor. The position relationship of the two flow holes on the static and dynamic valve plates is shown in Fig. 3.  $O_3$  is the center of the dynamic valve plate,  $O_4$  is the center of the eccentric hole on the dynamic valve plate,  $O_5$  is the center of the static valve plate, the circle  $O_3$  share the same axis with the circle  $O_4$  and is internally tangent with the circle  $O_4$ . At the initial time, the angle between the line  $O_4 O_3$  and the axis  $Y$  is  $120^\circ$ .

According to the analysis above, the motion equations of  $O_4$  are obtained by

$$\begin{cases} x_4 = e \sin \omega t + e_m \sin \left( \omega t + \frac{\pi}{6} \right) \\ y_4 = e \cos \omega t - e_m \cos \left( \omega t + \frac{\pi}{6} \right) \end{cases} \quad (8)$$

where  $e_m$  is the eccentricity of the eccentric hole relative to dynamic valve plate central axis, as the distance  $O_3 O_4$ . Defin-

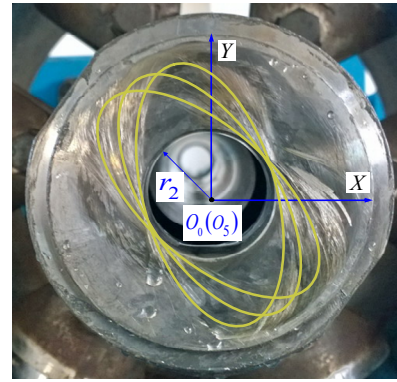


Fig. 4. Parameters relationship on the static valve plate.

ing  $r_0$  as the radius of dynamic valve plate,  $r_1$  as the radius of eccentric hole,  $r_0'$  as the radius of circle  $O_3$  and  $s$  as the difference between  $r_0$  and  $r_0'$ ,  $e_m$  can be described as

$$e_m = r_0 - r_1 - s. \quad (9)$$

To the static valve plate, the center of the flow hole and static valve plate is the same point. Defining  $O_5$  as the center of the flow hole on the static valve plate, the displacement between the eccentric hole  $O_4$  and  $O_5$  can be given by

$$\delta = \left[ e^2 + e_m^2 - 2e \cdot e_m \cdot \cos \left( 2\omega t + \frac{\pi}{6} \right) \right]^{\frac{1}{2}}. \quad (10)$$

The length of intersecting chord  $L$  is described as

$$L = \frac{1}{\delta} \left[ (r_1 + r_2 + \delta)(r_1 + r_2 - \delta)(r_1 + \delta - r_2)(r_2 + \delta - r_1) \right]^{\frac{1}{2}} \quad (11)$$

where the symbol  $r_2$  represents the radius of the flow hole on the static valve plate and the yellow lines represent the trajectory of the circle  $O_4$  on the static valve plate affected by the dynamic valve plate under the working conditions, as shown in Fig. 4.

Setting  $\theta_1$  and  $\theta_2$  as the central angles of  $L$  corresponding to  $O_4$  and  $O_5$ , its expressions are given by

$$\begin{cases} \theta_1 = 2 \arcsin \left( \frac{L}{2r_1} \right) \\ \theta_2 = 2 \arcsin \left( \frac{L}{2r_2} \right) \end{cases}. \quad (12)$$

According to the change of the intersecting chord  $L$  increasing from 0 to  $2r_1$ , then decreasing from  $2r_1$  to 0, the time symbols are defined as  $t_1 < t_2 < t_3 < t_4$ . Moreover, when  $r_1 \leq r_2$ ,  $t_1$  and  $t_4$  refer to the time  $L = 2r_2$ ,  $t_2$  and  $t_3$

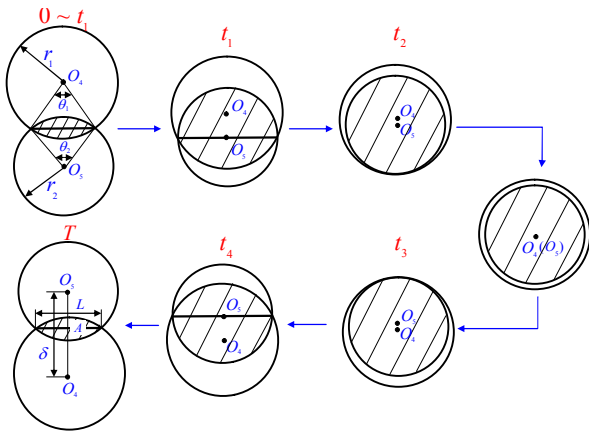


Fig. 5. Position changes of the circles  $O_4$  and  $O_5$ .

refer to the time  $L = 0$ . The motion characteristics between the circles  $O_4$  and  $O_5$  are in Fig. 5.

To the flow area  $A$  of drilling fluid, which is also the intersecting area of the two flow holes on static and dynamic valve plates, it is the basis for analyzing the energy conversion and drill string system vibration, and its expressions are, respectively, given by following:

When  $r_1 > r_2$

$$A = \begin{cases} \frac{1}{2}r_1^2\theta_1 + \frac{1}{2}r_2^2\theta_2 - \frac{1}{2}L\delta & \text{for } t \in (0, t_1) \cup (t_4, T) \\ \pi r_2^2 - \frac{1}{2}r_2^2\theta_2 + \frac{1}{2}r_1^2\theta_1 - \frac{1}{2}L\delta & \text{for } t \in (t_1, t_2) \cup (t_3, t_4) \\ \pi r_2^2 & \text{for } t \in (t_2, t_3). \end{cases} \quad (13)$$

Similarly, when  $n \leq r_2$

$$A = \begin{cases} \frac{1}{2}r_1^2\theta_1 + \frac{1}{2}r_2^2\theta_2 - \frac{1}{2}L\delta & \text{for } t \in (0, t'_1) \cup (t'_4, T) \\ \pi r_1^2 - \frac{1}{2}r_1^2\theta_1 + \frac{1}{2}r_2^2\theta_2 - \frac{1}{2}L\delta & \text{for } t \in (t'_1, t'_2) \cup (t'_3, t'_4) \\ \pi r_1^2 & \text{for } t \in (t'_2, t'_3) \end{cases} \quad (14)$$

where  $t'_1$  and  $t'_4$  refer to the time  $L = 2r_1$ ,  $t'_2$  and  $t'_3$  refer to the time  $L = 0$ ,  $T$  refers to the time cycle of the flow area  $A$ , and  $0 < t'_1 < t'_2 < t'_3 < t'_4 < T$ .

Besides when the PDM works in a circle, the flow area  $A$  will periodically change twice, just as shown in Fig. 5. So the angular velocity of the flow area  $A$  is

$$\omega_1 = \frac{2\pi}{T} = 2\omega. \quad (15)$$

### 2.3 Vibration analysis of drill string system

According to the drilling field conditions, with the analysis results of kinematic characteristics, the vibration model of the drill string system with the hydro-oscillator can be established. Setting the drilling well as horizontal, and the drill string and downhole tools (including hydro-oscillator) are elastic deformation in drilling process, the vibration model of the drill string system is established, as shown in Fig. 6.

In the analysis model, the symbol  $F_{sta}$  means the force upper drill string acting on BHA,  $F_{h-oscillator}$  is the axial harmonic force generated by the hydro-oscillator,  $F_{har1}$  is the harmonic force of drilling fluid acting on bit,  $F_{har2}$  is the axial force generated by the absorber,  $F_{bit}$  is the bit-rock interaction force, and  $m_i$  is the mass element of drill string,  $F_{fric}$  is the friction force between the drill string and borehole well,  $G_0$  is the BHA gravity,  $F_N$  is the support of the BHA.

With the symbol definitions above, according to the drilling field situation, the parameters relationship can be analyzed. Moreover, the vibration model can be described by

$$[\mathbf{M}]\ddot{\mathbf{u}}(t) + [\mathbf{C}]\dot{\mathbf{u}}(t) + [\mathbf{K}]\mathbf{u}(t) = \mathbf{F}_{sta} + \mathbf{F}_{h-oscillator}(t) + \mathbf{F}_{har1}(t) + \mathbf{F}_{har2}(t) + \mathbf{F}_{bit}(t) + \mathbf{F}_{fric} \quad (16)$$

where  $[\mathbf{M}]$  is the mass matrix,  $[\mathbf{C}]$  is the damping matrix,  $[\mathbf{K}]$  is the stiffness matrix, and  $u$  is the axial displacement of the drill string.

For the element  $k_i$  of the stiffness matrix, it can be calculated by following

$$k_i = \frac{E_i A_i}{l_i} \quad (17)$$

where  $E_i$  is Young's modulus,  $A_i$  is the element cross-sectional area, and  $l_i$  is the element length.

For the damping matrix, in drilling condition, it can be regarded as proportional to the mass matrix, and its calculation formula is as the following:

$$[\mathbf{C}] = \alpha[\mathbf{M}] + \beta[\mathbf{K}] \quad (18)$$

where  $\alpha$  and  $\beta$  are the scale factors,  $\alpha = 0.1$ ,  $\beta = 0.001$ .

According to the meaning of the symbols in the model above, the right-hand side of Eq. (16) represents the forces acting on the whole system, which can be obtained as the following.

The function of  $F_{har1}(t)$  is given by

$$F_{har1}(t) = F_0 \sin(\omega_h \cdot t) \quad (19)$$

where  $F_0$  and  $\omega_h$  are the amplitude and frequency of the harmonic force,  $\omega_h = \omega_1$ .

In terms of  $F_{har2}(t)$ , for the axial vibration produced by the

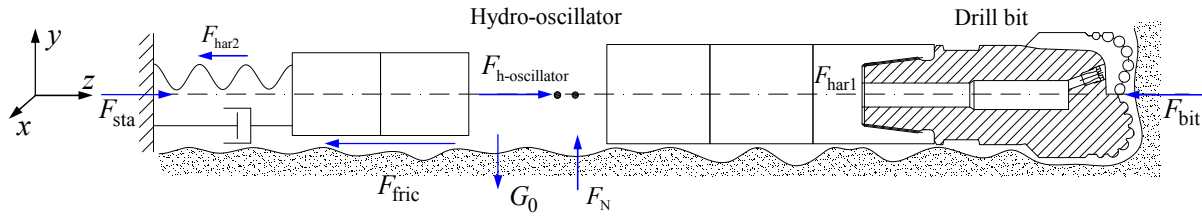


Fig. 6. Vibration analysis model of the hydro-oscillator.

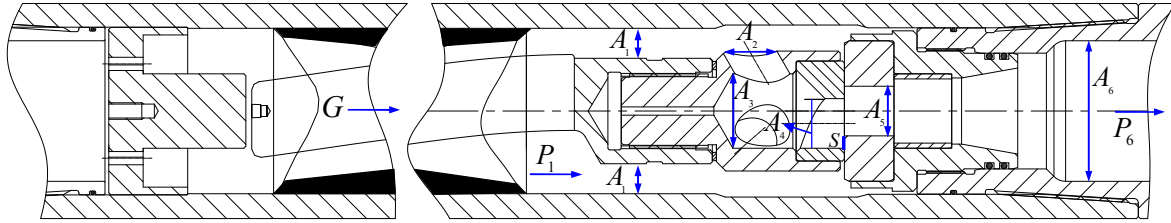


Fig. 7. Analysis of the axial harmonic force generated by the hydro-oscillator.

hydro-oscillator transmitting in two directions along the axis, the upward transmission of vibration will be translated into the downward vibration from the disc spring in the upper. The force generated by the tensile disc spring is

$$F_{har2}(t) = -K \cdot u(t) \tag{20}$$

where  $K$  is the disc spring stiffness,  $u(t)$  is the displacement of the hydro-oscillator.

According to the drill bit field situation,  $F_{bit}(\dot{u}(t))$  can be calculated by

$$\begin{cases} F_{bit}(\dot{u}(t)) = c_1 \exp(-c_2 \dot{u}(t)) - c_1 & \text{for } \dot{u}(t) > 0 \\ F_{bit}(\dot{u}(t)) = 0 & \text{for } \dot{u}(t) \leq 0 \end{cases} \tag{21}$$

where  $c_1$  and  $c_2$  are the constants of interaction between the bit and rock.

Among the parameters of the vibration model, the friction force between the drill string and borehole well is given by

$$F_{fric} = -\mu mg \cdot \text{sgn}(\dot{u}(t)) \tag{22}$$

where  $\mu$  is the friction coefficient,  $m$  is the BHA gravity quality,  $g$  is the gravitational constant.

Besides the above forces, there is still a very important force  $F_{h-oscillator}$  that should be taken into account in detail. As shown in Fig. 7, the analysis is presented about the axial harmonic force generated by the hydro-oscillator.

By the Bernoulli equation, the function of the pressure drop is given by

$$\begin{aligned} \bar{P}_n - \bar{P}_{n+1} &= \frac{1}{2} \rho (v_n^{-2} - v_{n+1}^{-2}) + \rho g h_{j(n+1)} \\ &= \frac{1}{2} \rho \left[ \left( \frac{Q}{A_n} \right)^2 - \left( \frac{Q}{A_{n+1}} \right)^2 \right] + \rho g h_{j(n+1)} \end{aligned} \tag{23}$$

where  $\bar{P}_n$  is the average pressure in section  $n$ ,  $\rho$  is the drilling fluid density,  $v_n$  is the average flow velocity in section  $n$ ,  $A_n$  is the flow area of section  $n$ ,  $h_{j(n+1)}$  is the local head loss from section  $n$  to section  $n+1$ .

The axial force generated by the changes of the flow area is

$$F_{har}(t) = \bar{P}_4 S = \bar{P}_4 (A_5 - A) \tag{24}$$

where  $\bar{P}_4$  is the average pressure in the eccentric hole of the dynamic valve plate;  $A_5 = \pi r_2^2$ ,  $r_2$  is the radius of the flow hole on the static valve plate;  $A$  is the intersecting area of the two flow holes on the static and dynamic valve plates.

The axial force of the PDM rotor is

$$G = G_3 + G_1 - G_2 = \xi G_3 = \xi \Delta p (\pi R^2 + 16ER) \tag{25}$$

where  $G_1$  is the axial force acting on the rotor when the liquid in the high pressure cavity leaks to the low pressure cavity,  $G_2$  is the part of the axial force caused when the eccentric screw (rotor) and fixed lining (stator) contact with friction, according to their helicoid along the axial movement,  $G_3$  is the part of the axial force caused by pressure drop  $\Delta p$  of the liquid between the high pressure port and the low pressure port,  $\xi$  is the axial force coefficient, taking  $\xi = 1$ ,  $R$  is the rotor radius.

Besides the two axial forces mentioned above, the axial force caused by the system pressure difference should also be considered; it can be obtained by approximate calculation

$$F_\Delta = (\bar{P}_1 - \bar{P}_6) A_6 \tag{26}$$

Therefore, the function of  $F_{h-oscillator}$  is given by

$$F_{h-oscillator} = F_{har}(t) + G + F_\Delta \tag{27}$$



Table 1. The example parameters of hydro-oscillator.

Parameter name	Result
Diameter of dynamic valve plate (mm)	55.32
Diameter of hole on rotor valve plate (mm)	27.94
Eccentricity of hole to rotor (mm)	10.084
Diameter of hole on static valve plate (mm)	30.48
Absorber stiffness (kN/mm)	4.5
Volumetric efficiency	0.95
Drilling fluid density (kg/m <sup>3</sup> )	1100
Pressure drop of the motor (MPa)	3.2
Rotor radius (mm)	40.589
Volumetric flow rate of drilling fluid (L/s)	22
Inputting pressure of drilling fluid (MPa)	20
Outer diameter of stator (mm)	80.594
Pitch of hydro-oscillator motor (mm)	530

### Numerical calculation and analysis

Depending on the analysis model and calculation formulas presented above, the numerical example can be discussed. With inputting parameters according to drilling field situation in a horizontal well, taking the size of the hydro-oscillator as the analysis object, the calculation results mainly include the hydro-oscillator vibration force, displacement, velocity and acceleration.

For the parameters of drilling in a horizontal well, the elastic modulus of the drill string  $E = 210$  GPa, its inside diameter  $D_i = 71.4$  mm, outside diameter  $D_o = 114.3$  mm, unit weight  $\rho_l = 63$  kg/m, element length  $l_i = 9.45$  m, gravity acceleration  $g = 9.8$  m/s<sup>2</sup>, friction coefficient  $\mu = 0.1$ ,  $c_1 = 1400$  N,  $c_2 = 400$ , PDM frequency  $\omega = 38.13$  rad/s,  $F_{sta} = 5500$  N,  $F_0 = 550$  N. The hydro-oscillator parameters are shown in Table 1.

Using the established calculation method, inputting the parameters above, the change curve of the drilling fluid flow area between the static and dynamic valve plates is obtained, as shown in Fig. 8. Simultaneously, the change of the axial force is shown in Fig. 9, caused by the hydro-oscillator in a cycle. Compared with Figs. 8 and 9, the change of the flow area is inversely proportionate to the axial force; with the decrease of the flow area, the axial force will increase. When the flow area decreases to the minimum, the axial force can increase to 34 KN, which could improve the efficiency of rock breaking for bits.

Moreover, from the figure shown, the axial force is a continuous and gentle sine-cosine fitting pulse, which can solve the problems of drill-string sticking and dragging, and improve the extension capacity of bits efficiently. On the other hand, the axial force is influenced not only by the continuing movement between the static and dynamic valve plates, but also by the pressure of the drilling fluid, which is the coupling results of the hydro-oscillator and drilling fluid.

Fig. 10 is the excitation spectrum generated by the hydro-

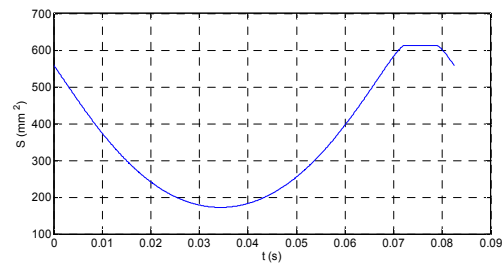


Fig. 8. Flow area between the static and dynamic valve plates.

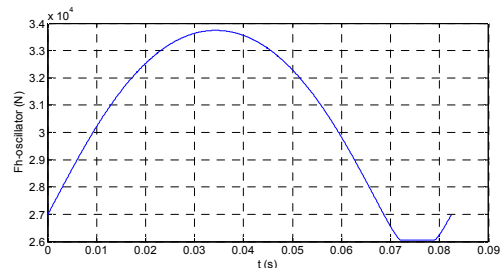


Fig. 9. Axial force caused by the hydro-oscillator.

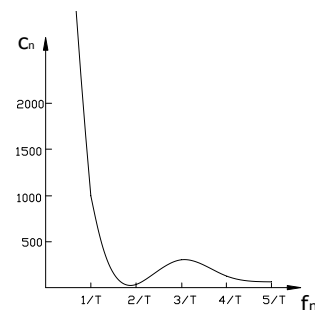
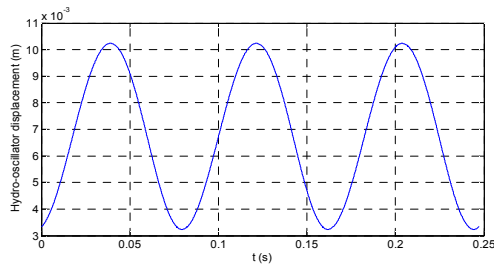


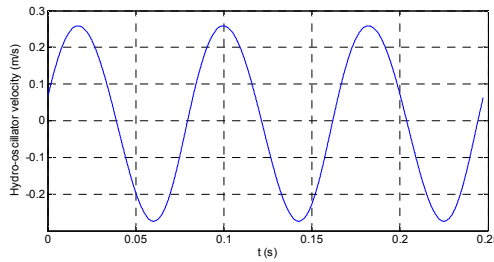
Fig. 10. Characteristics of excitation generated by the hydro-oscillator.

oscillator; for the axial harmonic force function could be expanded by the Fourier series. The numbers in the vertical coordinate refer to the amplitudes of different frequency, the fundamental wave amplitude (refers to  $1/T$ ) is greater than the other high order waves, all the high order wave amplitudes fluctuate in a small scope, which means that the axial harmonic force generated by the hydro-oscillator changes smoothly and the vibration waveform closes to the fundamental wave. In addition, according to the example parameters and formulas in Sec. 2.2, the hydro-oscillator vibration frequency is 12.14 Hz and its amplitude is small, so the hydro-oscillator vibration is a vibration with high frequency and micro amplitude, which has a remarkable effect on improving wall smoothness and reducing wellbore friction.

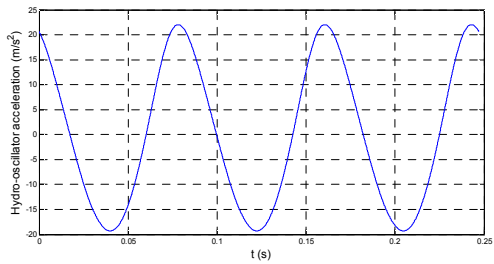
Taking the axial force results into vibration analysis model, the vibration characteristics of the hydro-oscillator can be obtained, including the displacement, velocity and acceleration shown in Fig. 11. Moreover, the displacement amplitude is about 3.7 mm, the velocity amplitude is about 0.25 m/s, and the acceleration amplitude is about 20 m/s<sup>2</sup> in three circles, which also proves the micro-amplitude vibration. Besides, the



(a) Displacement calculation results



(b) Velocity calculation results



(c) Acceleration calculation results

Fig. 11. Calculation results of vibration characteristics.

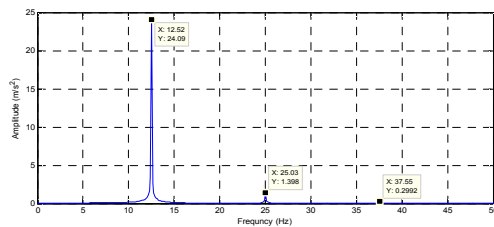


Fig. 12. Analytical response result of acceleration spectrum.

analytical result of acceleration response spectrum is calculated by Fast Fourier transform (FFT), the strong point of acceleration spectrum mainly concentrates on 12.52 Hz, which meets the excitation spectrum change rule.

### 3. Experiment test and analysis

To verify the correctness of the analysis model, corresponding to the numerical example parameters, an experiment test was conducted. The parameters of the hydro-oscillator were consistent with the numerical examples, as shown in Fig. 11. The experimental equipment included the downhole tool, plunger pumps, hydro-oscillator, absorber, test-sensor, throttle valves, inlet and outlet pipes. Each test lasted two minutes.

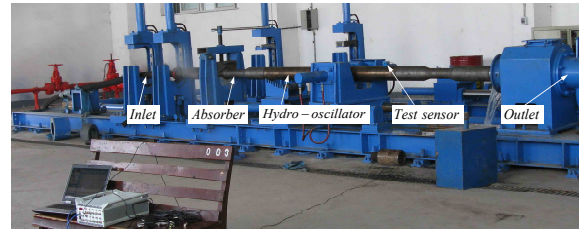


Fig. 13. Hydro-oscillator bench test.

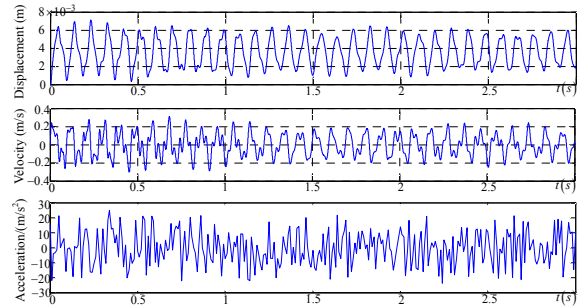


Fig. 14. Displacement, velocity and acceleration results of experiment test.

According to the experiment test results shown in Fig. 14, the displacement, velocity and acceleration were obtained during 0~3 seconds. When the mud pump flow rate kept 22 L/s, the axial vibration displacement of the hydro-oscillator was about 3~4 mm, the velocity was about 0.2~0.25 m/s, and the acceleration was about 18~20 m/s<sup>2</sup>, which was consistent with the numerical calculation results, as shown in Fig. 11.

Furthermore, the vibration parameters, especially for the velocity and acceleration, fluctuated up and down to a certain extent, which was due to the effects of some uncertainty force, such as the frictional force between the drill string and test bench, or the unstable hydraulic shock force of drilling fluids.

Fig. 15 is the experimental test of the hydro-oscillator axial force, the American BDI (strain measuring device) was used to test the axial force spectrum. Four strain gages were installed to the connecting rods on the test bench. Before the force testing, pre-pressure was applied and the four specimen EA was tested. When the hydro-oscillator was working, the axial force could be transferred to the four rods, so the axial force generated by the hydro-oscillator could be tested through the rod force. From Fig. 15(c) shown, the frequency points are mainly distributed from 10.8 Hz to 12 Hz, which meets the analytical results in Sec. 3.

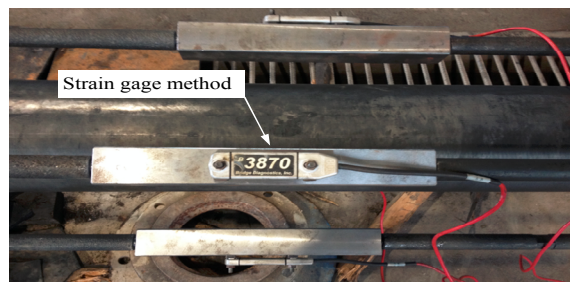
### 4. Conclusions

By analyzing the movement of the hydro-oscillator and the results of axial harmonic force, a vibration analysis model of a new drill string system is established, and its vibration characteristics in a horizontal well are analyzed. The following conclusions can be obtained:

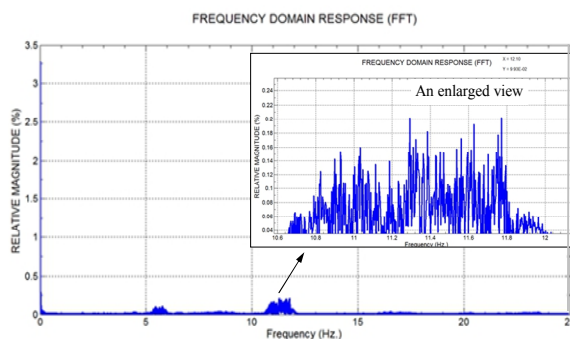
- (1) Based on the theoretical analysis and test results, the



(a) Bench test of axial force



(b) Specimen strain change with time



(c) Drawing of axial force spectrum

Fig. 15. Experimental test of axial force spectrum.

change of the flow area is inversely proportionate to the axial force; the hydro-oscillator could produce a vibration with high frequency and micro amplitude.

(2) The continuous and gentle vibration effects will turn the static friction between the drill string and wellbore to dynamic friction. Owing to the friction-reduced in the drilling process, it can result in a significant increase in ROP and run length.

(3) By adjusting the corresponding parameters according to the operation conditions, the analysis method and model can also be applied to similar drilling tool or technology research, and provide references to the study of downhole tools dynamics or mechanical properties under new complex drilling conditions.

## Acknowledgments

This work is supported by Open Fund (OGE201403-05) of Key Laboratory of Oil & Gas Equipment, Ministry of Education (Southwest Petroleum University), National Natural Science Foundation of China (No.51074202, No.11102173) and Major Cultivation Foundation of Sichuan Education Depart-

ment (12ZZ003, No.667).

## Nomenclature

$q$	: Flow quantity of per revolution
$A_s$	: Sectional area of stator
$A_r$	: Sectional area of rotor
$N$	: Rotor lobes
$e$	: Rotor eccentricity value
$D_r$	: External diameter of stator
$h$	: Motor screw pitch
$R$	: Rotor radius
$\omega$	: Rotation angular velocity of rotor around its center
$Q$	: Total flow rate
$\eta$	: Flow efficiency
$e_m$	: Eccentricity of the eccentric hole relative to dynamic valve plate central axis
$A$	: Flow area of drilling fluid
$T$	: Time cycle of the flow area
$r_0$	: Radius of dynamic valve plate
$r_1$	: Radius of eccentric hole

## References

- [1] A. A. Bond et al., Reliable technology for drilling operations in a high-pressure/high-temperature environment, *SPE*, 167972 (2014).
- [2] J. Pyecroft, S. Merkle and J. Lehmann, Second generation testing of cased uncemented multi-fractured horizontal well technology in the Horn River, *SPE*, 1925131 (2014).
- [3] R. Gee et al., Axial oscillation tools vs. lateral vibration tools for friction reduction – What's the best way to shake the pipe, *SPE*, 173024 (2015).
- [4] S. Tarasov, A. Kolubaev and S. Belyaev, Study of friction reduction by nanocopper additives to motor oil, *Wear*, 252 (1) (2002) 63-69.
- [5] H. Zhang et al., A novel tool to improve rate of penetration-down-hole drilling string absorption & hydraulic supercharging device, *SPE*, 176559 (2015).
- [6] M. Okada et al., Cutting characteristics of twist drill having cutting edges for drilling and reaming, *JMST*, 28 (5) (2014) 1951-1959.
- [7] J. L. Tian et al., Rock-breaking analysis model of new drill bit with tornado-like bottomhole model, *JMST*, 29 (4) (2015) 1745-1752.
- [8] D. Xuecheng et al., Study on running characteristic of oscillation impactor for oil-drilling, *J. of Mechanical Engineering*, 50 (21) (2014) 197-205.
- [9] H. Storck, W. Littmann and J. Wallaschek, The effect of friction reduction in presence of ultrasonic vibrations and its relevance to travelling wave ultrasonic motors, *Ultrasonics*, 40 (1) (2002) 379-383.
- [10] V. C. Kumar and I. M. Hutchings, Reduction of the sliding friction of metals by the application of longitudinal or transverse ultrasonic vibration, *Tribology International*, 37 (10)

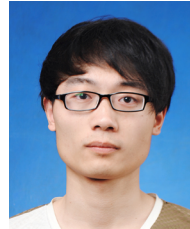


(2004) 833-840.

- [11] P. Wang, H. J. Ni and Z. N. Li, A modified model for friction reduction by vibrating drill-string longitudinally, *Applied Mechanics and Materials*, 535 (2014) 597-601.
- [12] A. S. Yigit and J. Kamel, Modeling and analysis of axial and torsional vibration of drillstrings with drag bits, *SPE*, 17258 (2014).
- [13] T. Richard, C. Germay and E. Detournay, A simplified model to explore the root cause of stick-slip vibration drilling systems with drag bits, *J. of Sound and Vibration*, 305 (2007) 432-456.
- [14] X. Hao et al., Hydraulic oscillators in a new gas field Shinsa 21-28H well applications, *Gas Industry*, 33 (3) (2013) 64-67.
- [15] D. Xuecheng et al., Numerical simulation analysis of rock breaking mechanism for oscillation impactor, *J. of Southwest Petroleum University*, 36 (6) (2014) 160-167.
- [16] L. P. Skyles, Y. A. Amiraslani and J. E. Wilhoit, Converting static friction to kinetic friction to drill further and faster in directional holes, *SPE*, 151221 (2012).
- [17] J. A. González, Partitioned vibration analysis of internal fluid-structure interaction problems, *International J. for Numerical Methods in Engineering*, 92 (3) (2012) 268-300.
- [18] G. Huagao, Effects of friction on post-buckling behavior and axial load transfer in a horizontal well, *SPE Journal*, 15 (4) (2012) 1104-1118.



**Jialin Tian** is currently an associate professor at School of Mechanical Engineering, Southwest Petroleum University. His research interests include the mechanical dynamics, drill bit technology, downhole tools, and drilling dynamics.



**Zhi Yang** is currently a graduate student at School of Mechanical Engineering, Southwest Petroleum University. His research interests include downhole tools and drilling dynamics.



**Lin Yang** received her Ph.D. in Mechanical Engineering from Southwest Petroleum University in 2013. She continued her postdoctoral research at the School of Petroleum Engineering, Southwest Petroleum University. Her research interests include drilling dynamics and hydromechanics.